López Gresa, MP.; Torres Vidal, C.; Campos Beneyto, L.; Lisón Párraga, MP.; Rodrigo Bravo, I.; Belles Albert, JM.; Conejero Tomás, V. (2011). Identification of defence metabolites in tomato plants infected by the bacterial pathogen Pseudomonas syringae. Environmental and Experimental Botany. 74:216-228. doi:10.1016/j.envexpbot.2011.06.003.

Identification of defence metabolites in tomato plants infected by the bacterial pathogen *Pseudomonas syringae*

María Pilar López-Gresa, Cristina Torres, Laura Campos, Purificación Lisón, Ismael Rodrigo, José María Bellés*, Vicente Conejero

Instituto de Biología Molecular y Celular de Plantas (IBMCP). Universidad Politécnica de Valencia (UPV)-Consejo Superior de Investigaciones Científicas (CSIC).

Ciudad Politécnica de la Innovación (CPI) Ed. 8E.

C/ Ingeniero Fausto Elio s/n, 46022 Valencia, Spain

*Corresponding author: Tel: +34963877880; Fax: +34963877859

E-mail address: jmbelles@btc.upv.es

Postal address: Instituto de Biología Molecular y Celular de Plantas (IBMCP). Universidad Politécnica de Valencia (UPV)-Consejo Superior de Investigaciones Científicas (CSIC). Ciudad Politécnica de la Innovación (CPI) Ed. 8E. C/ Ingeniero Fausto Elio s/n, 46022 Valencia, Spain

ABSTRACT

In the present work, we aimed to define the chemical nature of the phenylpropanoids induced during the interaction of the tomato plant, cultivar Rutgers, with the bacterial pathogen *Pseudomonas syringae* pv. *tomato.* Using LC-MS and NMR spectroscopy, we determined the chemical structures of this class of metabolites, which accumulated in response to exposure to the pathogen. A rapid accumulation of phytoalexin hydroxycinnamic acid amides (HCAA) of noradrenaline (*cis/trans N-p*-coumaroylnoradrenaline and *cis/trans N*-feruloylnoradrenline) and octopamine (*cis/trans N-p*-coumaroyloctopamine and *cis/trans N*-feruloyloctopamine), chlorogenic acid (CGA), and the flavonoid rutin was detected after bacterial infiltration. Among them, *cis N-p*-coumaroylnoradrenaline, *cis N-p*-coumaroyloctopamine, and isomers *cis/trans* of *N*-feruloylnoradrenaline have never been described in the literature. Moreover, *cis/trans* isomers of *N*-feruloyloctopamine are identified for the first time as being associated with the tomato/*P. syringae* interaction. Inhibition of the *P. syringae*-induced ethylene by 2-aminoethoxyvinylglycine, markedly impaired the accumulation of HCAA in inoculated tomato leaves, but it had no effect on CGA or rutin synthesis. On the other hand, the lack of accumulation of SA in NahG transgenic tomato plants, overexpressing a bacterial salicylic hydroxylase, did not prevent the enhancing of HCAA produced by *P. syringae* infection. Taken together, our results indicate that ethylene, but not SA, is essential for the synthesis of HCAA in response to bacterial infection of tomato leaves. Antibiotic activities of the induced metabolites were also studied. CGA induced a notable expression of the defence-related genes *PR1* and *P23*. Moreover, *trans*-HCAA of noradrenaline and octopamine showed a potent free radical scavenging competence. In particular, *trans N*-feruloylnoradrenaline presented a very

outstanding antioxidant activity, thus indicating that these compounds may play a role in the defence response of tomato plants against bacterial infection.

50

Keywords: Solanum lycopersicum, Pseudomonas syringae, plant metabolites, plant-pathogen interactions, hydroxycinnamic acid amides, free radical scavenging activity.

1. Introduction

The lack of mobility of higher plants prevents them from escaping of a wide array of damaging agents, including biotic (viroids, viruses, bacteria, fungi or nematodes) and abiotic (drought and salinity) environmental challenges. To cope with this continuous threat, plants have evolved very efficient and polyvalent biochemical defence mechanisms to provide an adequate and efficient response. Consequently, successful infection is difficult and the norm, rather than the exception, is that many plants are resistant to pathogens. Plants responses involve physical and chemical barriers, including active defence reactions that impede the invasion (Dangl and Jones, 2001; Dixon, 2001; Daayf et al., 2003).

Plant defence responses also include activation of the phenylpropanoid pathway leading to the synthesis of a remarkably vast array of low-molecular-mass natural chemicals characteristic of many cellular regulatory processes in plant physiology known as secondary metabolites. These compounds can provide protection against environmental changes and biotic or abiotic stresses (Dixon, 2001; Jahangir et al., 2009). Evidence has emerged during the past decades demonstrating the importance of products from the phenylpropanoid pathway in plant defence response against pathogens (Dixon et al., 2002; Jahangir et al., 2009). In recent years, very extensive and detailed studies on changes of metabolites in plant tissues have been carried out in some plant pathogen interactions such as Arabidopsis/*Pseudomonas syringae* (Hagemeier et al., 2001; Tan et al., 2004), tobacco/*tobacco mosaic virus* (Choi et al., 2006) or saskatoons/*Entomosporium mespili* (Wolski et al., 2010). However, less is known regarding changes of the metabolic profile associated with the response of tomato plants to pathogens (Bednarek et al., 2004; Zacarés et al., 2007).

The first key step in the biosynthesis of plant phenylpropanoid compounds is carried out by the enzyme phenylalanine ammonia-lyase (PAL; EC 4.3.1.5), which catalyses the deamination of L-alanine to *trans*-cinnamic acid (phenylpropenoic acid). The second reaction is regulated by cinnamate 4-hydroxylase (C4H; EC 1.14.13.11), which catalyses the hydroxylation of *trans*-cinnamic acid to *p*-coumaric acid (4-hydroxycinnamic acid) (Schilmiller et al. 2009). The hydroxycinnamic acids *p*-coumaric and ferulic (4-hydroxy-3-methoxycinnamic acid) serve as precursors for a wide variety of chemically diverse phenylpropanoid derivatives with antimicrobial functions, such as the plant-specific phytoalexin hydroxycinnamic acid amides (HCAA) and flavonoids (Dixon et al., 2002; Facchini et al., 2002).

In previous studies (Fayos et al., 2006; Zacarés et al., 2007; Bellés et al., 2008; López-Gresa et al., 2010), we have determined the chemical structure, accumulation kinetics, and functional significance of diverse compounds from the phenylpropanoid metabolism in tomato and cucumber infected with different pathogens. In particular, challenging Rutgers tomato with *P. syringae pv. tomato*, a bacterial pathogen of tomato and Arabidopsis, rapidly induced the expression of the hydroxycinnamoyl-CoA:tyramine hydroxycinnamoyltransferase (*THT*) gene, coding for the key enzyme responsible for the synthesis of hydroxycinnamoyl amides. Notably, and in agreement with this increase, a substantial accumulation of hydroxycinnamoyl amides of dopamine with positive antibacterial and antioxidative effects was detected (Zacarés et al., 2007).

To complement our previous studies on the characterization and functional significance of secondary metabolites accumulation during the interaction between Rutgers tomato and *P. syringae*, here we focus on the structural elucidation and antimicrobial function of compounds that may be components of tomato chemical defence responses against pathogens.

2. Materials and methods

2.1. Maintenance of plants and inoculation procedure

Seeds from tomato (*Solanum lycopersicon* cultivar Rutgers) (Western Hybrid Seeds Inc., Hamilton City, CA, U.S.A.), transgenic tomato plants overexpressing the bacterial SA hydroxylase transgene (*NahG* gene) (Brading et al., 2000) or from MoneyMaker (the isogenic parental line for NahG), kindly provided by Professor J.D.G. Jones (John Innes Centre, Norwich, U.K.), were used in this study. Experimental lots of 20 plants from each cultivar of uniform morphological and physiological conditions were prepared for each experiment. Plants were grown in 20-cm-diameter pots containing a mixture of peat and vermiculite (1:1, w/w). The pots were subirrigated once a day with a nutrient Hoagland solution as previously described (Bellés et al. 2006). Growth conditions in the greenhouse were ambient lighting supplemented by metal halide (Osram Powerstar 400 w HQI-BT/D Daylight E40) and sodium vapour (Philips MASTER SON-T PIA 400 w E40) lamps during 16 h photoperiod (7500 lux), and 27/23 ºC (day/night) with a relative humidity ranging from 60% (day) to 85% (night). Five-week-old Rutgers, transgenic NahG or MoneyMaker tomato plants at the five- to six-leaf stage were used in all the experiments described in this work. Infection of plants was done with a bacterial suspension of *Pseudomonas syringae* pv. *tomato* DC 3000 obtained by growing bacteria from a glycerinated suspension overnight at 28 ºC in Petri dishes with 20 ml sterilized LB broth medium supplemented with 100 µl riphampicine (50 mg ml^{-1}). Bacterial colonies were then transferred to 15 ml LB liquid medium and grown overnight at 28º C. Bacteria were pelleted by centrifugation and resuspended in

10 mM $MgSO_4$ to an optical density of 0.1 at 600 nm. Dilution plating was used to calculate the inoculum concentration, which averaged 10^7 CFU ml^{-1}. The third and fourth leaves from five-week-old plants were inoculated with *P. syringae* according to the procedure previously described in detail (Collinge et al., 1987). Briefly, aliquots of 100 µl of inoculum per inoculation were injected via the stomata into the abaxial side of each five leaflets with a 1-ml sterilized plastic syringe without needle. Five panels per leaflet as uniform as possible averaging 50 mm^2 were inoculated. Mock inoculations of control plants were performed similarly in equivalent leaflets with a sterile solution of 10 mM $MgSO_4$.

2.2. General experimental procedures

Silica gel chromatography was performed using pre-coated Merck F_{254} plates and silica gel 60, 0.06-0.2 mm powder. Optical rotations were measured on a Jasco DIP 370 digital polarimeter. UV measurements were obtained using a Shimadzu UV-2101PC spectrophotometer. ^1H, ^{13}C, and ^1H-^1H COSY NMR spectra were recorded on a Bruker AV 300 MHz instrument. Multiplicities of ^{13}C signals were assigned by DEPT experiments. For HSQC and HMBC NMR experiments a Bruker DRX-600 spectrometer, operating at 600 MHz for ^1H and 150 MHz for ^{13}C using an inverse TCI CryoProbe fitted with a gradient along the Z-axis, was used. High resolution ESI-MS data were obtained on a Micromass Q-TOF Micro™ coupled with a UPLC Aquity. The source parameters of the mass spectrometer for ESI in negative mode were the following: capillary voltage 3 kV, cone voltage 35 V, extraction cone 0.5 V, RF Lens1 0.9 V, RF Lens2 6 V, source block temperature 120 ºC and desolvation gas temperature 300 ºC. The desolvation and cone gas used was nitrogen at a flow rate of 650 l/h and 50

l/h, respectively. Other mass spectrometer conditions were: low mass resolution 5, high mass resolution 5, ion energy 0.2, and collision energy 10. ESI data acquisition was in the conditions of a full scan range from mass-to-charge ratio [*m/z*] 50 to 1.500 at 0.2 s per scan. The instrument was calibrated using a PEG mixture from 200 to 1500 MW (resolution specification 5000 FWHM, deviation <5 ppm RMS in the presence of a known lock mass).

2.3. Extraction procedure and HPLC/ESI-MS analysis of secondary metabolites

The third and fourth leaves from control mock-inoculated and *Pseudomonas syringae*-infected tomato plants were harvested at the appropriate time points after inoculation, combined, immediately finely powdered in liquid nitrogen in a mortar with a pestle and stored at -80 ºC until use. An aliquot of 0.5 g of leaf powder mixture from each plant sample was transferred to a mortar and homogenised with 1.5 ml of methanol. The extraction mixture was vortexed for 1 min, and then sonicated for 10 min and centrifuged at 14000g for 15 min in an Eppendorf bench centrifuge to remove cellular debris. The pellet was resuspended in 1 ml of methanol, and the same steps were repeated as above. Both supernatants (total volume 2.5 ml) were transferred to 5-ml glass tubes and dried under a flow of nitrogen at 40 ºC. The residue was dissolved in 500 µl of methanol and filtered through 13 mm Nylon 0.45 µm Minispike filters (Waters). The solvent was evaporated and the residue dissolved again in 100 µl of methanol. All steps of the extraction were performed under dark conditions to avoid *cis/trans* light-induced isomerization of phenylpropanoid double bonds (Muhlenbeck et al., 1996). A 20 µl aliquot from the final 100 µl sample was injected into an analytical reverse-phase Sun Fire 5 µm C18 column (4.6 x 150 mm, Waters) equilibrated in 1 %

acetic acid at 25 ºC. Eluents were 1 % acetic acid (eluent A) and methanol (eluent B). A linear gradient starting with 100 % eluent A and 0 % eluent B was applied over 20 min at a flow rate of 1 ml min^{-1} was applied with a Waters 1525 HPLC binary pump connected to a Waters 2996 UV photodiode array detector (PDA). After washing the column with 100 % methanol for 5 min, the initial conditions were again applied and the column was allowed to equilibrate with 1 % acetic acid for 10 min. A post-PDA split delivered ca. 25 % of the flow to a Waters ZMD mass spectrometer equipped with an electrospray ionization (ESI) source. The source parameters of the mass spectrometer for ESI in negative and positive mode were the following: capillary voltage 2500 V, cone voltage 20 V (negative mode) or 30 V (positive mode), extractor 5 V (negative mode) or 7 V (positive mode), RF Lens 0.5 V, source block temperature 100 ºC and desolvation gas temperature 300 ºC. The desolvation and cone gas used was nitrogen at a flow rate of 300 l h^{-1} and 50 l h^{-1}, respectively. Other mass spectrometer conditions were: low mass resolution 13.5 (negative mode) or 16.6 (positive mode), high mass resolution 13.5 (negative mode) or 16.6 (positive mode), ion energy 0.5 (negative mode) or 0.2 (positive mode), and multiplier 650. ESI data acquisition was in the conditions of a full scan range from mass-to-charge ratio [*m/z*] 100 to 800 at 1 s per scan. Compounds were quantified from the data recorded and analysed with the Masslynx Waters software by constructing standards curves with authentic synthesised standards.

2.4. Extraction and isolation of compounds **2A** and **4A**

Frozen *P.syringae*-infected tomato leaves showing strong symptoms of the disease (60.5 g FW) were homogenized with a Heidolph homogenizer (Diax 900) in methanol

(500 ml). The extracts were maintained at 40 ºC with constant agitation in magnetic stirrer hotplates during 2 h, then sonicated for 15 min, and centrifuged at 14000 *g* for 15 min to remove cellular debris. The methanol from the supernatant (400 ml) was removed under vacuum, and the resulting aqueous suspension was successively extracted with hexane, ethyl acetate and 1-butanol. The three organic phases corresponding to hexane, ethyl acetate, and 1-butanol were concentrated by evaporating the organic solvent, and the dry residues (425 mg, 47.8 mg, and 305.9 mg, respectively) were dissolved in methanol (1 mg ml^{-1}). Twenty µl of each methanolic solution was injected into a Sun Fire 5 µm C18 column (4.6 x 150 mm, Waters) equilibrated in 1 % acetic acid at 25 ºC and analysed using the gradient explained above. Results showed that all the induced compounds characterised here (**1-6, 2A-5A**) were present in the ethyl acetate fraction. This organic fraction was submitted to silica gel column chromatography using a stepwise gradient of 3 ml each from hexane/ethylacetate (3/7) to methanol. Aliquots were pooled in 6 fractions according to their similarity by TLC and dried under vacuum. Fraction 2 (2.8 mg), eluted with hexane/ethylacetate (3/7), was used as source for purifying compound **4A** (retention time (RT) = 11.9 min) by HPLC (Shimadzu SCL-10A liquid chromatograph, equipped with a Shimadzu UV SPD-10A detector). Samples (20 µl) were injected into a Phenomenex Synergy Hydro-RP 80A, 4 µm (250 x 4.6 mm) equilibrated in MeOH/H_2O (0.1% TFA):25/75. A 20 min linear gradient starting with MeOH/H_2O (0.1% TFA):25/75 and ending with 100 % MeOH at a flow of 1 ml min^{-1} was applied. Several runs were performed and the total amount of collected compound **4A** was 0.6 mg. Fraction 3 (7.3 mg), eluted with ethyl acetate, was used to purify by HPLC compound **2A** (RT = 16.6 min), employing the same reverse-phase column and a 30 min linear gradient starting with MeOH/H_2O (0.1% TFA):10/90 and ending with 100 % MeOH. After doing several runs, the total collected amount of

compound **2A** was 0.5 mg. Under the last chromatographic condition, retention time of compound **4A** was 22.1 min.

2.5. Synthesis of *trans*-HCAA

Chemicals were obtained from commercial suppliers and used without further purification. Ferulic acid, *p*-coumaric acid, (±) octopamine hydrochloride, (–) noradrenaline, and *N,N'*-dicyclohexylcarbodiimide (DCC) were obtained from Sigma-Aldrich and *N,N*-dimethylformamide (DMF) was from Panreac. The identified *trans*-HCAA were synthesized by condensation of *p*-coumaric and ferulic acids with both (-) noradrenaline and (±) octopamine (hydrochloride form) in the presence of DCC, as dehydrating agent following the method described by Tanaka et al. (1989). Briefly, to a mixture of the corresponding hydroxycinnamic acid (0.5 mmol) and amine (0.65 mmol) dissolved in DMF (20 ml), a solution of DCC (0.8 mmol) in DMF (5 ml) was added, and the reaction mixture stirred overnight at room temperature. After removal of the solvent, the reaction mixture was diluted with a large volume of H_2O and extracted with ethyl acetate. The upper organic layer was dried over Na_2SO_4 and evaporated to dryness to give viscous oil, which was purified by a column of silica gel 60 (0.06-0.2 mm) equilibrated with a mixture of hexane/ethyl acetate 1:1 as the mobile phase. Fraction 5, eluted with 100% ethyl acetate, was used to purify synthesised compounds by preparative reverse-phase HPLC (Waters 600E) at room temperature under isocratic conditions using a mixture of MeOH and 1% acetic acid (25:75) at a flow rate of 10 ml min^{-1}. Samples (100 µl) were injected onto a SymmetryPrep 7 µm C18 column (19 x 150 mm, Waters) and the synthesised compounds were photometrically detected with a Waters 996 PDA detector. Several runs were carried out and the total amount of

collected HCAA was approximately 5 mg of each one. Under these experimental conditions, retention times of synthesized HCAA were the following: 18.4 min for compound **2** (*trans*-CNA), 24.8 min for compound **3** (*trans*-FNA), 32.1 min for compound **4** (*trans*-CO), and 35.4 min for compound 5 (*trans*-CNA). All the synthetic compounds were identical to bacterial induced metabolites in tomato leaves, as judged by comparison of their retention times in the analytical HPLC chromatograms as well as UV and MS spectra.

2.6. AVG and ethylene treatments of Rutgers tomato plants

For AVG and ethylene treatments, 5-week-old Rutgers tomato plants were used. AVG treatments were performed in the greenhouse under the same conditions employed for growing plants. Third and fourth leaves from Rutgers tomato were sprayed until run-off with 1 mM aqueous solution of AVG containing 0.05 % Tween 20 as a wetting agent and treatment was repeated after 10 h. Two hours later, the AVG-treated leaves were inoculated with the bacterial suspension. The inoculated leaves were excised at the indicated times to analyse secondary metabolites. For comparison, equivalent tomato leaves mock inoculated with 10 mM $MgSO_4$ were used as controls. Ethylene treatments were carried out on Rutgers tomato plants placed during 24 h into 125 litre sealed containers in a controlled environment growth chamber at 25 ºC under a 16-h photoperiod (5000 lux). A mixture of ethylene (50 µl l^{-1}) in air (Linde) was passed through the containers at a constant flow rate of 15 l h^{-1}. Control tomato plants were placed in an equivalent environment growth chamber with a 15 l h^{-1} flow rate of air without ethylene. At 24 h, third and fourth Rutgers tomato leaves were collected to determine metabolites.

2.7. Preparation and analysis of RNA

The accumulation of mRNAs for phenylalanine ammonia-lyase (*PAL*), hydroxycinnamoyl CoA quinate transferase (*HQT*) and cinnamate 4-hydroxylase (*C4H*) was analysed by Northern blot. Total RNA was extracted using the TRIzol reagent (Gibco BRL) and 15 μg of total RNA were electrophoresed in 1.2% agarose gels in the presence of formaldehyde, then transferred to Nytran membranes and hybridized using standard procedures. DNA probes were obtained by RT-PCR. Primers for PAL and HQT were designed from their published tomato sequences (Lee et al., 1992; Niggeweg et al., 2004). C4H primers were designed from the nucleotide sequence described for *Capsicum annuum* (accession number AF088847). The following oligonucleotides were used: PAL forward (5'-CAAGGGCTGGTGTGAAAGC-3') and reverse (5'-GTCCTTCCTTGGGCTGCAAC- 3'); HQT forward (5'-GAGTCGCTCTTGGTGGTGGA-3') and reverse (5'-CATCTAGACAAACAGCCAAACGC- 3'); C4H forward (5'-TTACGGTTTATGGTGAGCATTGG-3') and reverse (5'-CACAATGTTGTTTGCATTGCAG- 3'). Radioactive DNA probes were prepared using the RediPrime II labelling kit (GE Healthcare). Hybridizations and high stringency washes were performed as described by Church and Gilbert (1984).

2.8 Induction of pathogenesis related defence genes by CGA

The third and fourth leaves from Rutgers tomato were used to study the effect of CGA on the induction of the defence-related genes *PR1* and *P23*. CGA was applied by

immersing the petioles of excised leaves in a Falcon 50 ml tube containing 40 ml of an aqueous solution of 1 mM CGA. Equivalent leaves immersed in water, instead of 1 mM CGA, were used as controls. At the specified times after inoculation or treatments, leaves from *P. syringae*-infected and mock-inoculated Rutgers tomato plants, as well as 1 mM CGA-treated and control plants were collected. Total RNA was extracted using the TRIzol reagent (Gibco BRL), and 10 µg RNA was reverse-transcribed with 100 U of M-MLV reverse transcriptase (Promega) at 37 ºC for 60 min in a volume of 50 µl, using a 18-mer oligo (dT) as a primer. Five µl of reverse-transcribed cDNA was amplified by PCR using standard procedures with the following conditions: 1 min of denaturation at 94 ºC followed by 25 cycles of 1 min of denaturation at 94 ºC, 1 min of annealing at 55 ºC and 1 min of extension at 72 ºC, finished with an extension step of 5 min at 72 ºC. The oligonucleotide primers used to amplify tomato *PR1* mRNA (Tornero et al., 1993) were 5'-CACTAAACCTAAAGAAAAATGG-3' (forward) and 5'-GTGGAATTATTCATATTAGC-3' (reverse). For tomato *P23* mRNA (Rodrigo et al., 1993), the oligonucleotides were: 5'-GACTTACACTTATGCTGCC-3' (forward) and 5'-TATATTAGGTTTATTACAAGCC-3' (reverse). Aliquots of 25 µl of the PCR products were electrophoresed on 1 % agarose gels, stained with ethidium bromide and visualized under UV light. Accumulation of the tomato ribosomal *RPL2* mRNA (Fleming et al., 1993) was used as a loading control with the following oligonucleotide primers: 5'-GGTGACCGTGGTGTCTTTGC-3' (forward) and 5'-ACCAACCTTTTGTCCAGGAGGT-3' (reverse).

2.9. Antioxidant activity

Free radical scavenging activity of induced HCAA after bacterial infection and their

hydroxycinnamic acids and β-phenylethyl-amines, as well as that of natural antioxidant compounds, was evaluated using the assay based on the scavenging of the stable radical 2,2-diphenyl-1-picrylhydrazyl (DPPH) (Hirota et al., 2000). This method is based on the reduction of alcoholic DPPH solutions at 517 nm in the presence of an antioxidant compound. Two millilitres of ethanolic solution containing the corresponding compounds at different concentrations were mixed with 1 ml of 0.5 mM DPPH (dissolved in ethanol) and 2 ml of 0.1 M sodium acetate (pH 5.5). After incubation of the mixture at 25 °C for 30 min, the absorbance at 517 nm was measured using a Pharmacia Biotech 1000E UV-VIS spectrophotometer. Radical scavenging activity was expressed as the concentration of product necessary to reduce to 50% the absorbance of DPPH at 517 nm (ED_{50}). Butylated hydroxytoluene (BHT) was tested as a positive control.

2.10. Compound characterization

Analytical data were obtained from synthetic compounds (**2-5, 3A, 5A**) and isolated compounds (**2A, 4A**)

Compound **2**, *trans*-CNA**:** White powder; $[\alpha]_D^{25}$ +27.5° (c 0.69, MeOH); UV (MeOH) λ_{max} (log ε) 292 (0.78), 310 (0.75) nm; ^{1}H NMR (MeOH-d_4, 300 MHz) and ^{13}C NMR (MeOH-d_4, 75 MHz) see Table S2; HRESIMS *m/z* 314.0995 $[M-H]^-$ (calcd for $C_{17}H_{16}NO_5$, 314.1028).

Compound **2A**, *cis*-CNA: White powder; $[\alpha]_D^{25}$ +12.4° (c 0.14, MeOH); UV (MeOH) λ_{max} (log ε) 276 (0.86), 309 (0.60) nm; ^{1}H NMR (MeOH-d_4, 600 MHz) and ^{13}C NMR

(MeOH-d_4, 150 MHz) see Table S2; HRESIMS *m/z* 314.0999 $[M-H]^-$ (calcd for $C_{17}H_{16}NO_5$, 314.1028).

Compound **3**, *trans*-FNA**:** White powder; $[\alpha]_D^{25}$ +40.9° (c 1.1, MeOH); UV (MeOH) λ_{max} (log ε) 290 (1.10), 319 (1.25) nm; ^{1}H NMR (MeOH-d_4, 300 MHz); δ 7.45 (1H, *d*, *J*=15.7, H-7), 7.12 (1H, *d*, *J*=1.8, H-2), 7.02 (1H, *dd*, *J*=8.1, 1.8, H-6), 6.85 (1H, *d*, *J*=1.5, H-2'), 6.79 (1H, *d*, *J*=8.1, H-5), 6.76 (1H, *d*, *J*=8.2, H-5'), 6.73 (1H, *dd*, *J*=8.2, 1.5, H-6'), 6.46 (1H, *d*, *J*=15.7, H-8), 4.65 (1H, *dd*, *J*=7.7, 4.9, H-7'), 3.88 (3H, *s*, OCH_3), 3.52 (1H, *dd*, *J*=13.5, 4.9, H8'a), 3.42 (1H, *dd*, *J*=13.5, 7.7, H8'b); ^{13}C NMR (MeOH-d_4 75 MHz); δ 169.9 (C, C-9), 149.9 (C, C-4), 149.3 (C, C-3), 146.9 (C, C-3'), 146.3 (C, C-4'), 142.3 (CH, C-7), 135.6 (C, C-1'), 128.3 (C, C-1), 123.3 (CH, C-6), 118.8 (CH, C-8), 118.7 (CH, C-6'), 116.5 (CH, C-5), 116.2 (CH, C-5'), 114.5 (CH, C-2'), 111.6 (CH, C-2), 73.6 (CH, C-7'), 55.2 (-OCH_3), 47.2 (CH_2, C-8'); HRESIMS *m/z* 344.1118 $[M-H]^-$ (calcd for $C_{18}H_{18}NO_6$, 344.1134).

Compound **3A**, *cis*-FNA: UV (MeOH) λ_{max} (log ε) 279 (1.15), 306 (0.90) nm; HRESIMS *m/z* 344.1129 $[M-H]^-$ (calcd for $C_{18}H_{18}NO_6$, 344.1134).

Compound **4**, *trans*-CO**:** White powder; UV (MeOH) λ_{max} (log ε) 290 (1.18), 310 (1.20) nm; ^{1}H NMR (MeOH-d_4, 300 MHz); δ 7.45 (1H, *d*, *J*=15.8, H-7), 7.40 (2H, *d*, *J*=8.5, H-2 and H-6), 7.22 (2H, *d*, *J*=8.5, H-2' and H-6'), 6.78 (2H, *d*, *J*=8.5, H-3 and H-5), 6.76 (2H, *d*, *J*=8.5, H-3' and H-5'), 6.43 (1H, *d*, *J*=15.8, H-8), 4.72 (1H, *dd*, *J*=7.8, 4.9, H-7'), 3.53 (1H, *dd*, *J*=13.6, 4.9, H8'a), 3.42 (1H, *dd*, *J*=13.6, 7.8, H8'b); ^{13}C NMR (MeOH-d_4 75 MHz); δ 169.6 (C, C-9), 160.6 (C, C-4), 158.1 (C, C-4'), 142.0 (CH, C-7), 134.8 (C, C-1'), 130.6 (CH, C-2 and C-6), 128.5 (CH, C-2' and C-6'), 127.8 (C, C-

1), 118.4 (CH, C-8), 116.7 (CH, C-3 and C-5), 116.1 (CH, C-3' and C-5'), 73.5 (CH, C-7'), 48.3 (CH_2, C-8'); HRESIMS *m/z* 298.1050 $[M-H]^-$ (calcd for $C_{17}H_{16}NO_4$, 298.1079).

Compound **4A,** *cis*-CO**:** White powder; $[\alpha]_D^{25}$ +22.5° (c 0.19, MeOH); UV (MeOH) λ_{max} (log ε) 276 (1.20), 304 (1.05) nm; ^{1}H NMR (MeOH-d_4, 600 MHz); δ 7.41 (2H, *d*, *J*=8.2, H-2 and H-6), 7.21 (2H, *d*, *J*=8.2, H-2' and H-6'), 6.78 (2H, *d*, *J*=8.2, H-3 and H-5), 6.75 (2H, *d*, *J*=8.2, H-3' and H-6'), 6.64 (1H, *d*, *J*=12.4, H-7), 5.83 (1H, *d*, *J*=12.4, H-8), 4.68 (1H, *dd*, *J*=7.9, 5.4, H-7'), 3.45 (2H, *m*, H8'); HRESIMS *m/z* 298.1061 $[M-H]^-$ (calcd for $C_{17}H_{16}NO_4$, 298.1079).

Compound **5**, *trans*-FO**:** White powder; UV (MeOH) λ_{max} (log ε) 290 (1.60), 319 (1.85) nm; ^{1}H NMR (MeOH-d_4, 300 MHz); δ 7.44 (1H, *d*, *J*=15.7, H-7), 7.22 (2H, *d*, *J*=8.4, H-2' and H-6'), 7.12 (1H, *d*, *J*=1.8, H-2), 7.02 (1H, *dd*, *J*=8.2, 1.8, H-6), 6.79 (1H, *d*, *J*=8.2, H-5), 6.77 (1H, *d*, *J*=8.4, H-3' and H-5'), 6.46 (1H, *d*, *J*=15.7, H-8), 4.72 (1H, *dd*, *J*=7.8, 4.9, H-7'), 3.88 (3H, *s*, OCH_3), 3.53 (1H, *dd*, *J*=13.6, 4.9, H8'a), 3.43 (1H, *dd*, *J*=13.6, 7.8, H8'b); ^{13}C NMR (MeOH-d_4 75 MHz); δ 169.5 (C, C-9), 158.1 (C, C-4'), 149.9 (C, C-4), 149.3 (C, C-3), 142.3 (CH, C-7), 134.7 (C, C-1'), 128.5 (CH, C-2' and C-6'), 128.3 (C, C-1), 123.3 (CH, C-6), 118.6 (CH, C-8), 116.5 (CH, C-5), 116.1 (CH, C-3' and C-5'), 111.5 (CH, C-2), 73.5 (CH, C-7'), 56.4 (-OCH_3), 48.3 (CH_2, C-8'); HRESIMS *m/z* 328.1189 $[M-H]^-$ (calcd for $C_{18}H_{18}NO_5$, 328.1185).

Compound **5A**, *cis*-FO: UV (MeOH) λ_{max} (log ε) 274 (1.40), 302 (1.20) nm; HRESIMS *m/z* 328.1150 $[M-H]^-$ (calcd for $C_{18}H_{18}NO_5$, 328.1185).

3. Results and discussion

3.1. Detection and structural characterization of secondary metabolites in Rutgers tomato plants induced upon infection by *P. syringae*

Infiltration of tomato leaflets with *P. syringae* resulted in dry necrotic bronzed spots and cellular breakdown over the whole inoculated area at 72 hours after inoculation, and thereafter, the bacteria spread and produced yellow chlorotic spots in the adjacent non-inoculated zones. The HPLC chromatogram (retention time from 9 to 15 min) of a methanolic extract from *P. syringae*-infected tomato leaves at 24 h postinoculation revealed a complex pattern of eight major peaks named **1**-**8** (RT = 9.6, 11.3, 11.6, 11.8, 12.3, 13.2, 13.6, and 13.9 min, respectively), which were specifically induced or notably enhanced by the infection (Fig. S1A). Peaks **7** and **8** had been previously characterised in ethyl acetate extracts from Rutgers tomato inoculated with *P. syringae* as *p*-coumaroyltyramine and feruloytyramine, respectively (Zacarés et al., 2007).

The first step in the identification of peaks from the UV absorption chromatogram was carried out mainly using mass spectrometry. From the data of mass spectra, peak **1** was identified as chlorogenic acid (5-*O*-caffeoyl-quinic acid, CGA) (RT = 9.6 min) and peak **6** as the flavonoid glycoside rutin [quercetin (3,3',4',5,7-pentahydroxyflavone) β-3-*O*-rutinoside] (RT = 13.2 min). They were reproducibly induced in infected tomato tissues. Low basal levels of these compounds were also present in control leaves (Fig. S1A). CGA, one of the most abundant phenolic compounds in infected tomato leaves, showed the typical fragmentation pattern in negative ion mode: *m/z* 353 $[M - H]^-$, *m/z* 707 [2M - H], and *m/z* 191 $[M – \text{caffeoyl acid}]^-$ (Clé et al., 2008). The negative-ion spectrum of rutin showed the molecular ion *m/z* 609, and product ion spectra in the

positive ion mode was $[M + H]^+$ *m/z* 611, *m/z* 465, and *m/z* 303, the two last being the ion products formed by two successive losses of sugar residues (Fuentes-Alventosa et al., 2007). Identity of CGA and rutin was also confirmed by spiking a non-inoculated sample with authentic standards in different conditions of HPLC analysis. Recently, it has been found that rutin accumulated greatly in potato plants in response to *Verticillium dahliae* (El Hadrami et al., 2011).

To precisely identify the peaks **2**-**5**, an HPLC-MS analysis, combined with PDA detection and electrospray ionization (ESI) of the methanol-extractable compounds from *P. syringae*-infected tomato leaves was performed. Table S1 shows the mass spectra, under mild ionization conditions (cone voltage of 20 V), from total ion current chromatograms obtained by ESI in negative and positive ion mode, UV absorbance maxima, and HPLC retention times of peaks **2**-**5**. $(M-H)^-$ fragment ions of mass-to-charge ratio (*m/z*) equal to 314 (RT = 11.3 min), 344 (RT = 11.6 min), 298 (RT = 11.8 min), and 328 (RT = 12.3 min) were detected by ESI in negative mode (Table S1). Unexpectedly, reconstructed single ion chromatograms from total ion current of each *m/z* species gave more that one peak. Both *m/z* species of 314 and 344 gave one additional peak with a retention time of 10.2 (peak **2A**) and 10.4 (peak **3A**) min, respectively. In addition, two new peaks were found as associated with both the *m/z* species of 298 (RT = 10.6 (peak **4A**) and RT = 12.9 (peak **9**) min), and 328 (RT = 10.8 (peak **5A**) and RT = 13.0 (peak **10**) min) (Fig. S1B). Peaks **9** and **10** corresponded to *p*-coumaroyldopamine and feruloyldopamine, which had been previously characterized in the same plant-pathogen interaction (Zacarés et al., 2007).

Table S1 also shows the mass spectra fragments of peaks **2**-**5** and **2A**-**5A** from soluble methanol tomato extracts obtained by ESI in the positive ion mode. Under these experimental conditions, the compounds gave a substantial fragmentation. The mass

spectra from total ion current chromatograms showed protonated $[Mh+H]^+$ fragment ions of a mass-to-charge [*m/z*] ratio equal to 316, 346, 300, and 330. The product ion scan spectrum of peaks **2**-**5** and **2A**-**5A** gave common ions at *m/z* 147 and 177, which are daughter ions, characteristic of the *p*-coumaroyl and feruloyl moieties, respectively. The UV absorption spectra were typical of HCAA and the molecular weight of the amine moieties coincided with those of the amines noradrenaline (norepinephrine, 2-hydroxy-2-[3,4-dihydroxyphenyl] ethylamine), octopamine (2-hydroxy-2-[(4-hydroxyphenyl] ethylamine) and dopamine (2-[3,4-dihydroxyphenyl] ethylamine). Moreover, the mass spectra also displayed a prominent $[M+H-H_2O]^+$ ion that was characteristic of the amine conjugates with a hydroxyl function at carbon 7 of the aliphatic chain from the amine moiety (Schmidt et al., 1999; Von Roepenack-Lahaye et al., 2003), which is the case of octopamine and noradrenaline. Thus, the information based on the mass spectra confirmed noradrenaline and octopamine as the amine conjugated in the putative *p*-coumaric and ferulic derivative HCAA. We synthesised the four *trans*-*p*-coumaric and *trans*-ferulic noradrenaline and octopamine amides from commercially available *trans*-*p*-coumaric and *trans*-ferulic acids, noradrenaline and octopamine. The elution times, UV absorption spectra, and ESI-MS spectra of peaks **2**-**5** were identical to those of authentic synthesised *trans*-*N*-*p*-coumaroylnoradrenaline (*trans*-CNA) (**2**), *trans*-*N*-feruloylnoradrenaline (*trans*-FNA) (**3**), *trans*-*N*-*p*-coumaroyloctopamine (*trans*-CO) (**4**), and *trans*-*N*-feruloyloctopamine (*trans*-FO) (**5**), and co-chromatographed with standards under different HPLC eluent conditions, thus unambiguously confirming the proposed chemical structures for peaks **2**-**5** (Table S1).

Compounds **2A** and **4A** reproducibly accumulated in infected tissues at amounts sufficient for their isolation and structural elucidation by ESI-MS, and 1D and 2D NMR spectroscopy. Compounds corresponding to peaks **3A** and **5A** were much less abundant,

making impossible their structural analysis. ESI-MS spectra from pairs of peaks **2** and **2A**, **3** and **3A**, **4** and **4A**, and **5** and **5A**, were indistinguishable, but the UV absorption spectra were markedly different, suggesting that peaks **2A-5A** are the *cis*-isomer of peaks **2-5**. This possibility was unequivocally confirmed by the ^{1}H-NMR signals of isolated compounds **2A** (Table S2) and **4A** for the olefinic protons on C7 and C8, doublets with J=12.6 Hz, indicative of a *cis*-double bond (King and Calhoun, 2005; Baker et al., 2005). Therefore, the proposed structure for **2A** and **4A** is *cis*-*N*-*p*-coumaroylnoradrenaline (*cis*-CNA) and *cis*-*N*-*p*-coumaroyloctopamine (*cis*-CO), respectively. The structure of compounds **3A** and **5A** was established by UV isomerisation of *trans*-chemical standards (Muhlenbeck et al., 1996), and were assigned as *cis*-*N*-feruloylnoradrenaline (*cis*-FNA) and *cis*-*N*-feruloyloctopamine (*cis*-FO), respectively. In general, *trans*-isomers are the most common in nature. Although maximum precautions have been taken, it cannot be ruled out that a small part of the *cis*-isomers found here were formed during the extraction procedure by factors like temperature or UV light.

As we observed the presence of a chiral centre in the eight HCAA analyzed, we have determined the optical activity of isolated compounds **2A** and **4A**. Both isolated compounds *cis*-CNA (**2A**) and *cis*-CO (**4A**) showed $[\alpha]_D^{25}$ +12.4° (c 0.14, MeOH) and $[\alpha]_D^{25}$ +25.5° (c 0.19, MeOH), respectively. The optical rotation of R- *trans*-CNA (**2**), synthesised from *p*-coumaric acid and the (-) (R) isomer noradrenaline, was $[\alpha]_D^{25}$ +27.5° (c 0.69, MeOH). Matsuda et al., (2000) also found a positive optical rotation ($[\alpha]_D^{25}$ +17.4° (c 1.0, H_2O) for *trans*-CO synthesised from (-) (R) isomer octopamine . Taking into account all these results, we propose that the HCAA formed by conjugation to noradrenaline and octopamine have the absolute configuration R. Moreover,

505 structurally-related β-hydroxyphenylethylamines, such as macromerine, described as plant constituents, have also been reported as R isomers (Brown et al., 1972).

To our knowledge, this is the first evidence of the presence of *cis*-CNA (**2A**), *cis*-FNA (**3A**), *cis*-CO (**4A**), and *trans*-FNA (**3**) in plants. Moreover, induction of *cis*-FO (**5A**), and *trans*-FO (**5**) had not been previously implicated in the interaction of Rutgers
510 tomato leaves with the bacterial pathogen *P. syringae* pv. *tomato.*

3.2. Accumulation of HCAA, chlorogenic acid, and rutin in Rutgers tomato leaves after infection with *P. syringae*

515 Figure 1 depicts the accumulation of *cis*/*trans* isomers of CNA, FNA, CO, and FO in Rutgers tomato leaves upon *P. syringae* infection monitored at 24 and 48 h (Fig. 1A), and that of CGA and rutin at 4, 24 and 48 h after inoculation of the leaves (Fig. 1B). No appreciable induction of HCAA could be detected at 4 h after inoculation, and the increased pool size of HCAA at 24 h did not significantly differ from those present at
520 48 h after inoculation. These results suggested that that major HCAA synthesis occurred early, during the first 24 h after bacterial infiltration. All of the HCAA were not present in mock-inoculated leaves during 48 h experiment. The level of these metabolites in bacteria infiltrated tomato leaves differed substantially depending on HCAA, with the highest values corresponding to *trans*-HCAA. In general, at 24 and 48 h
525 postinoculation, the pool size of HCAA derived from *trans*-*p*-coumaric acid, *trans*-CO (ca. 25 nmol g^{-1} FW) and *trans*-CNA (ca. 60 nmol g^{-1} FW), showed the highest levels when comparing with *trans*-feruloyl amides: *trans*-FO (ca. 9 nmol g^{-1} FW) and *trans*-FNA (ca. 11 nmol g^{-1} FW). On the other hand, all of the *cis*-HCAA accumulated to lower amounts than those of *trans*-HCAA, with the exception of the novel *cis*-CNA,

530 which reached a relatively high level (ca. 25 nmol g^{-1} FW) at 48 h after inoculation (Fig. 1A). After 48 h, the levels of all HCAA substantially decreased until day 5 postinoculation.

CGA and rutin are the most abundant phenolics constitutively present in tomato foliage. In Rutgers tomato, their basal levels ranged from 40 nmol to 60 nmol g^{-1} FW
535 and a slow but significant induction, particularly for rutin, occurred in mock-inoculated leaves, probably as a consequence of the injury due to the inoculation method (Fig. 1B). Both CGA and rutin began to substantially accumulate earlier than HCAA, and at 4 h postinoculation, their levels were significantly higher than those of mock-inoculated leaves (Figs. 1A and 1B). Levels of CGA and rutin in infected leaves progressively
540 increased until 48 h, and appreciably decreased until day 5 after infiltration (data not shown). It is interesting to emphasize for all the induced metabolites that their synthesis and accumulation took place during the first 24 h, well before the appearance of necrotic brown spots and the death of inoculated tissues, which were not visible until 72 h after infiltration of leaflets. Together, these results support the idea that these
545 phenolics may not be end products of the pathological process, but factors that could play a biological role in the initial response of tomato against bacterial attack. The relative timing of accumulation of the presently described HCAA in Rutgers tomato leaves infected with *P. syringae* was almost the same as that displayed for another class of HCAA, such as tyramine and dopamine derivatives, previously found in the same
550 plant pathogen interaction (Zacarés et al., 2007). In this context, it is interesting to compare the results from Von Roepenack-Lahaye et al. (2003) and ours in tomato with those obtained in potato infected with *Phytophthora infestans* or exposed to an elicitor preparation from the same fungus (Schmidt et al. 1999): neither noradrenaline nor octopamine HCAA were observed in the soluble methanol fraction from potato leaves,

555 and only *trans*-CO and *trans*-FO were reported as cell wall phenolic constituents in infected or elicitor-treated cell cultures of potato. Geometric *cis/trans* isomers of FO have been recently characterized in suberized potato tissues (King and Calhoun, 2005). In summary, the results emphasise and extend the biological role that HCAA could play in a successful plant defence to pathogens as previously suggested by others (Newman
560 et al., 2001; Von Roepenack-Lahaye et al., 2003). On the other hand, the rapid elevation of CGA and rutin after infiltration of leaves with bacteria suggests a possible protective effect of these compounds against pathogen infection. This idea is in agreement with what has been previously discussed regarding their potential role on the Verticillium wilt control in potato plants (El Hadrami et al., 2011).

565 Interestingly, a comparison of the results obtained in tomato infected with *P. syringae* with analogous data in *Arabidopsis thaliana*, shows remarkable differences in terms of the chemical structures of the induced substances. Two types of aromatic compounds include those derived from phenylalanine, common in the plant kingdom (phenylpropanoid branch pathway), and the structurally related tryptophan-derived
570 compounds, which are more specific to the *Brassicaceae* family (Hagemeier et al., 2001). Representative phenylpropanoid HCAA are chemicals prominently present in members of the *Solanaceae* species after pathogen infection or elicitor treatments (Keller et al., 1996; Schmidt et al., 1999). In particular for tomato, results of Von Roepenack-Lahaye et al. (2003) and those reported here, indicate that tomato plants
575 challenged with *P. syringae* mainly accumulated HCAA of tyramine, dopamine, octopamine and noradrenaline while, at least under our experimental conditions, no tryptophan-related or indolic substances were detected. Conversely, all the major accumulating soluble metabolites in leaves of Arabidopsis infected with *P. syringae* have been structurally identified as indolic tryptophan-related substances with the

concomitant absence of phenylalanine derived metabolites (Hagemeier et al., 2001). The diversity of Arabidopsis and tomato responses reflects the distinctive endowment of secondary compounds in each plant species.

3.3. Enhanced salicylic acid accumulation in *P. syringae*-infected tomato leaves is not a necessary signal for the detected induction of secondary metabolites

Compelling evidence had led to the conclusion that SA is an important intermediary signal in the activation of certain plant defence responses to biotic and abiotic stress agents (Delaney et al., 1994). It was demonstrated (Zacarés et al., 2007), that infection of Rutgers tomato with *P. syringae* resulted in a rapid (ca. 4 h after inoculation) and sharp induction of SA that clearly preceded the accumulation of HCAA found here (24-48 h after inoculation). This posed the question of whether the pathogen-enhanced level of SA could act as a signal to induce the accumulation of HCAA after infection. To correlate the presence of SA with the induction of these metabolites, transgenic NahG tomato plants harbouring a bacterial salicylate hydroxylase which eliminates SA by converting it to catechol (Brading et al., 2000), were infected with *P. syringae*. Analysis of methanolic extracts from *P. syringae*-infected NahG tomato plants revealed an induction pattern for all HCAA qualitatively similar to that of Rutgers, but differed quantitatively with increments more or less pronounced depending on the HCAA (Figs. 1A and 2A). No detectable levels of HCAA were found in mock-inoculated control plants. These results indicate that the induction of HCAA upon infection with *P. syringae* follows a signalling pathway which is independent of SA.

The induction pattern of CGA and rutin in transgenic NahG tomato was comparable to that of Rutgers either in mock-inoculated or infected with *P. syringae* (Figs. 1B and 2B). All these

results further suggested that SA is not implicated in the induction of these metabolites and their accumulation is also independent of SA. Interestingly, the behaviour of SA in transgenic NahG Arabidopsis was different. Nawrath and Métraux (1999) demonstrated that SA acted as a critical signal for the induction of the major phytoalexin camalexin upon *P. syringae* infection.

3.4. Enhanced ethylene synthesis in *P. syringae*-infected tomato leaves plays a role in the induction of HCAA

Enhanced formation of the gaseous plant hormone ethylene is a prominent and early response of plants to the recognition of invading pathogens or abiotic stresses (Díaz et al., 2002; Van Loon et al., 2006). It has been postulated that ethylene may play a role as a signal for activating plant defence reactions against pathogens. Two observations, based both on previously reported results (Reinhardt et al., 1991) and other presented here, prompted us to search for the possible role of endogenous ethylene on HCAA induction observed here: a) Rutgers tomato leaves produced a rapid (ca. 4 h after inoculation) and sharp elevation of ethylene synthesis upon infection with *P. syringae* (Bellés et al., 1999), which preceded accumulation of metabolites that occurred at 24-48 h postinoculation, and b) although with lower increments than in *P. syringae*-infected leaves, HCAA were also found to be substantially elicited 24 h after application of 50 µl l^{-1} exogenous ethylene (Fig. 3A), while CGA and rutin strongly and rapidly (4 h after treatment) augmented in response to the same ethylene treatment (Fig. 3B). HCAA were absent in non-treated control plants.

Therefore, an obvious question was whether or not the induced endogenous ethylene could, in turn, be a necessary signal for the subsequent accumulation of HCAA, CGA and rutin in response to bacterial infection. To test this, we treated tomato leaves with 1

mM 2-aminoethoxyvinylglycine (AVG), a specific chemical inhibitor of ethylene biosynthesis in higher plants. Previous experiments indicated that AVG markedly prevented the rapid burst of ethylene synthesis in *P. syringae*-infected tomato tissues (Zacarés et al., 2007). Importantly, the initial induction of HCAA was decreased (ca. 70-80%) in *P. syringae*-infected tomato leaves that had been pretreated with AVG 24 h before (Fig. 4). For all HCAA, the inhibitory effect of AVG at 48 h was much less pronounced as compared with that produced at 24 h after its application (Fig. 4). These results indicate that ethylene, produced after bacterial infection, is crucial for HCAA accumulation and are in agreement with the essential role of ethylene as a signal in tomato to respond to pathogen attacks (Lund et al., 1998). In contrast, no effect of AVG either on CGA or rutin induction was observed (data not shown), thus indicating that ethylene did not seem to play a major role in the accumulation of these metabolites in tomato after *P. syringae* infiltration.

3.5. Association of HCAA, CGA and rutin with gene expression alteration of phenylalanine ammonia-lyase, cinnamate 4-hydroxylase and hydoxycinnamoyl-CoA quinate: hydroxycinnamoyl transferase by *P. syringae*

Phenylalanine ammonia-lyase (PAL), the first key enzyme of the plant phenylpropanoid pathway, is well known to be induced after different infections such as tobacco leaves and soybean cells infected with tobacco mosaic virus (Pellegrini et al., 1994) or *P. syringae* (Delledonne et al., 1998), respectively. To correlate the elevated levels of metabolites found in *P. syringae*-infected leaves with the expression pattern of PAL, RNAs from mock-inoculated and infected tomato leaves were subjected to Northern analysis, using the PAL sequence as probe. Figure 5 presents the early

accumulation of transcripts coding for PAL at 4 h that remained until 24 h after inoculation of tomato leaves. This increase was transient and returned to very low levels by 48 h. PAL gene expression clearly preceded HCAA accumulation and correlated with CGA and rutin biosynthesis. Similarly, a rapid and transient induction of PAL activity was also observed in the necrotic reaction of cucumber plants against *P. syringae* pv. *syringae* infiltration (Smith-Becker et al., 1998), although in this interaction, PAL activity correlated with an increment of phenolic 4-hydroxybenzoic acid. In two compatible interactions, cucumber/prunus necrotic ring spot virus and melon/melon necrotic spot virus, an induction of PAL gene expression was also observed, but occurred at later time points (Bellés et al., 2008).

The increment of PAL gene expression levels seems to be coordinated with the induction of the gene encoding cinnamate 4-hydroxylase (C4H), the second key enzyme of phenolic metabolism (Chapple, 1998). A fast induction of C4H transcripts occurred 4 h after bacterial infection followed by a progressive decrease by 24 and 48 h (Fig. 5). Previous reports showed that the mRNA coding for C4H was rapidly and strongly induced in alfalfa and Arabidopsis roots infected with fungi *Phoma medicaginis* (He and Dixon, 2000) and *Pythium sylvaticum* (Bednarek et al., 2005), respectively. Here we show a direct correlation between elevated expression of C4H and the levels of rutin upon infection of tomato leaves with *P. syringae* (Figs. 1 and 5), thus suggesting that C4H could play a role in the accumulation of rutin. This agrees with reports on tobacco and tomato plants with altered expression of C4H also showing a concomitant direct modification of rutin levels (Blount et al., 2000; Millar et al., 2007).

Hydroxycinnamoyl-CoA quinate:hydroxycinnamoyl transferase (HQT) has been found to be the crucial enzyme which enables the synthesis of CGA in tobacco and tomato plants (Hoffmann et al., 2003; Niggeweg et al., 2004). A noticeable increment

680 above the control basal levels of HQT gene expression occurred at 4 h in inoculated leaves that remains constant at 24 h followed by a notable decrease and return to basal levels at 48 h after injection of the bacterial suspension (Fig. 5). Moderate or low basal levels of PAL, C4H or HQT transcripts were detected in control plants during 48 h experiment, which is consistent with the fact that they are key enzymes for 685 phyenylpropanoid metabolism. Results revealed a close correlation between the induction of HQT gene expression and the synthesis of CGA in *P. syringae*-infected tomato leaves. The two early key enzymes of phenylpropanoid pathway, PAL and C4H, and also HQT are strongly and concomitantly activated after infection by *P. syringae*. In this context, it is worthy to emphasize that their induction upon bacterial infection is 690 even more rapid than that of the defence key marker PR1 (Fig. 5).

Results presented here show that altered gene expression patterns, as a consequence of bacterial infection, involve three early key enzymes of plant secondary pathway, thus complementing our previous results in tomato that described THT as the induced enzyme catalysing the final step in the synthesis of elicited HCAA after infection of 695 tomato plants with *P. syringae* (Zacarés et al., 2007). Together, these results contrast with those found in Arabidopsis upon infection with the bacterial pathogen *P. syringae,* which demonstrated activation of the camalexin and thryptophan branch pathway (Niyogi and Fink, 1992), whereas we show here that the same pathogen activated genes from the phenylpropanoid branch pathway such as PAL, C4H, and HQT.

700

3.6. Induction of defence-related genes by CGA in Rutgers tomato leaves

The rapid synthesis of rutin and CGA in tomato infected leaves (4 h after bacterial inoculation) might indicate that these metabolites could act as endogenous signals

capable of eliciting antibiotic responses in infected tissues, i.e., synthesis of host defence-related proteins (Linthorst, 1991). Therefore, it was of interest to explore the possibility that exogenous addition of rutin and CGA would induce the expression of resistance marker P1 and P23 genes in tomato (Rodrigo et al., 1993; Tornero et al., 1993). An elevation of CGA of 180 nmol g^{-1} FW after exposing leaves to 1 mM CGA soln., comparable to the amount of CGA accumulated in bacterially infected leaves, led to an early induction of *PR1* transcripts that seems to reach a maximum 24 h after the beginning of the treatment. Likewise, *P23* transcripts also accumulated at 24 h, but no appreciable induction of *P23* gene expression was detected at 4 h. No detectable accumulation of the expression of these genes was observed after identical treatment of the leaves with rutin. Importantly, the CGA-mediated induction of *PR1* is faster than that observed for the induction time of *PR1* in response to *P. syringae* infection in Rutgers tomato leaves (Figs. S2A and S2B), or in the UC82B tomato infected with *Xanthomonas campestris* pv. *vesicatoria* (Block et al., 2005)23. Although CGA exhibited a potent *in vitro* induction of P1 and P23 genes, further studies need to examine whether CGA plays some defensive role in the tomato-*P. syringae* interaction.

3.7. The novel metabolite feruloylnoradrenaline possesses a strong antioxidant activity

Secondary induced compounds were analyzed for their antioxidant capacity by determining their 2,2-diphenyl-1-picrylhydrazyl (DPPH) free radical scavenging activity. The DPPH method was chosen because it is simple and accepted worldwide for the comparison of antioxidant activities of diverse natural antioxidants. Alcoholic oxidized DPPH was reduced by the antioxidant assayed and its decrease was followed measuring the absorbance at 517 nm. Previous reports have dealt with the importance of

HCAA as antioxidants and their importance as protector against accumulation of reactive oxygen species in plants after pathogen infection. Importantly, the novel HCAA characterized in the present work, *trans*-FNA, possessed the highest free radical scavenging activity among the induced secondary metabolites (7.92 μM), and was much higher than that of the synthetic antioxidant butylhydroxytoluene (BHT) control (61.13 μM) extensively used in the food industry to avoid undesirable oxidations (Table S3).

The activity of FNA was also considerably higher than that of CNA, previously characterized as a novel HCAA in plants (Von Roepenack-Lahaye et al., 2003) that also presented a notable antioxidant capacity ca. two times higher than that of BHT. The antiradical activities of octopamine conjugates were lower than that of noradrenaline (CO >200 μM; FO 81.11 μM) (Table S3). From these results, it was concluded that anti-DPPH radical activities of HCAA were well correlated with the presence of noradrenaline in the HCAA molecule. Comparison antioxidant activities of hydroxycinnamic acids and β-phenylethyl-amines revealed that antiradical activity of ferulic acid (44.92 μM) was notably higher than that of *p*-coumaric acid (>200 μM), whereas antioxidant activity of noradrenaline (24.1 μM) was drastically higher than that of octopamine (>200 μM) (Table S3). As previously described, the natural antioxidants, CGA and rutin, had notable antiradical competence as compared with that of BHT. Interestingly, the aglycone quercetin had a potent antiradical capacity higher than the glucoside, thus indicating that, most likely, quercetin is responsible for the radical scavenging capacity of rutin. For comparison, we investigated the free radical scavenging activity of the well-known potent natural antioxidant compounds (vitamins A and E) or phenolics (gentisic acid or resveratrol). Notably, the antioxidant capacity of FNA was much higher than any of these compounds.

Induction of potent antioxidants, such as FNA, could constitute a mechanism of cellular protection to prevent or scavenger the initial burst of reactive oxygen species upon exposure of tomato leaves to bacteria. Alternatively, accumulation of these compounds could protect plants acting directly against aspiring new pathogens. In this context, given the very potent free radical scavenging activity of *trans*-FNA, it would be interesting to generate tomato plants with elevated levels of this compound. Following a similar strategy carried out for THT and tyrosine decarboxylase (TYDC) (Hagel and Facchini, 2005; Kang et al., 2009), the two final key enzymes of HCAA metabolism, work is now in progress to engineer tomato plants with enhanced activity of both the THT and TYDC enzymes in order to explore whether *trans*-FNA accumulates. If this strategy is successful, these transgenic tomato plants would be useful to investigate the role of *trans*-FNA in tomato pathogen interaction and as an *in vivo* antipathogenic compound.

Acknowledgements

The authors want to thank Dr. Lynne Yenush for critical reading of the manuscript and exciting intellectual discussions. Dominique Melck, Estrella Mateos (ICB and ITQ NMR Service) for recording NMR spectra and Letizia Ciavatta for interpretation of the 600-MHz NMR spectra. This work was supported by Grant BFU2006-11546 from Dirección General de Programas y Transferencia de Conocimiento, from Spanish Ministry of Science and Innovation. M.P.L.G. was the recipient of a postdoctoral fellowship APOSTD/2007/128 from Generalitat Valencia (Spain).

Appendix A. Supplementary data

Supplementary data associated with this article can be found, in the online version.

References

Baker, C.J., Whitaker, B.D., Roberts, D.P., Mock, N.M., Rice, C.P., Deahl, K.L., Aver'yanov, A.A., 2005. Induction of redox sensitive extracellular phenolics during plant-bacterial interactions. Physiol. Mol. Plant Pathol. 66, 90-98.

Bednarek, P., Schneider, B., Svatos, A., Oldham, N.J., Hahlbrock, K., 2005. Structural complexity, differential response to infection, and tissue specificity of indolic and phenylpropanoid secondary metabolism in Arabidopsis roots. Plant Physiol. 138, 1058-1070.

Bednarek, P., Winter, J., Hamberger, B., Oldham, N.J., Schneider, B., Tan, J., Hahlbrock, K., 2004. Induction of 3'-*O*-β-D-ribofuranosyl adenosine during compatible, but not during incompatible, interactions of *Arabidopsis thaliana* or *Lycopersicon esculentum* with *Pseudomonas syringae* pathovar tomato. Planta 218, 668-672.

Bellés, J.M., Garro, R., Fayos, J., Navarro, P., Primo, J., Conejero, V., 1999. Gentisic acid as a pathogen-inducible signal, additional to salicylic acid for activation of plant defenses in tomato. Mol. Plant-Microbe Interact. 12, 227-235.

Bellés, J.M., Garro, R., Pallás, V., Fayos, J., Rodrigo, I., Conejero, V., 2006. Accumulation of gentisic acid as associated with systemic infections but not with the hypersensitive response in plant-pathogen interactions. Planta 223, 500-511.

Bellés, J.M., Lopez-Gresa, M.P., Fayos, J., Pallas, V., Rodrigo, I., Conejero, V., 2008. Induction of cinnamate 4-hydroxylase and phenylpropanoids in virus-infected cucumber and melon plants. Plant Sci. 174, 524-533.

Block, A., Schmelz, E., O'Donnell, P.J., Jones, J.B., Klee, H.J., 2005. Systemic acquired tolerance to virulent bacterial pathogens in tomato. Plant Physiol. 138, 1481-1490.

Blount, J.W., Korth, K.L., Masoud, S.A., Rasmussen, S., Lamb, C., Dixon, R.A., 2000. Altering expression of cinnamic acid 4-hydroxylase in transgenic plants provides evidence for a feedback loop at the entry point into the phenylpropanoid pathway. Plant Physiol. 122, 107-116.

Brading, P.A., Hammond-Kosack, K.E., Parr, A., Jones, J.D.G., 2000. Salicylic acid is not required for Cf-2- and Cf-9-dependent resistance of tomato to *Cladosporium fulvum*. Plant J. 23, 305-318.

Brown, S.D., Reinecke, M.G., Hodgkins, J.E., 1972. Isolation, structure, synthesis, and absolute configuration of cactus alkaloid macromerine. J. Org. Chem. 37, 773-775.

Chapple, C, 1998. Molecular-genetic analysis of plant cytochrome P450-dependent monooxygenases. Annu. Rev. Plant Physiol.Plant Mol. Biol.49, 311-343

Choi, Y.H., Kim, H.K., Linthorst, H.J.M., Hollander, J.G., Lefeber, A.W.M., Erkelens, C., Nuzillard, J.M., Verpoorte, R., 2006. NMR metabolomics to revisit the tobacco mosaic virus infection in *Nicotiana tabacum* leaves. J. Nat. Prod. 69, 742-748.

Church, G.M., Gilbert, W., 1984. Genomic sequencing. Proc Natl Acad Sci U. S. A. 81, 1991-1995.

Clé, C., Hill, L.M., Niggeweg, R., Martin, C.R., Guisez, Y., Prinsen, E., Jansen, M.A.K., 2008. Modulation of chlorogenic acid biosynthesis in *Solanum lycopersicum*; consequences for phenolic accumulation and UV-tolerance. Phytochemistry 69, 2149-2156.

Collinge, D.B., Milligan, D.E., Dow, J.M., Scofield, G., Daniels, M.J., 1987. Gene expression in *Brassica campestris* showing a hypersensitive response to the incompatible pathogen *Xanthomonas campestris* pv vitians. Plant Mol. Biol. 8, 405-414.

Daayf, F., El Bellaj, M., El Hassni, M., J'Aiti, F., El Hadrami, I. 2003. Elicitation of soluble phenolics in date palm (*Phoenix dactylifera*) callus by *Fusarium oxysporum* f. sp. *albedinis* culture medium. Environ. Exp. Bot. 49, 41-47.

Dangl, J.L., Jones, J.D.G., 2001. Plant pathogens and integrated defence responses to infection. Nature 411, 826-833.

Delaney, T.P., Uknes, S., Vernooij, B., Friedrich, L., Weymann, K., Negrotto, D., Gaffney, T., Gutrella, M., Kessmann, H., Ward, E., Ryals, J., 1994. A central role of salicylic acid in plant-disease resistance. Science 266, 1247-1250.

Delledonne, M., Xia, Y.J., Dixon, R.A., Lamb, C., 1998. Nitric oxide functions as a signal in plant disease resistance. Nature 394, 585-588.

Díaz, J., ten Have, A., Van Kan, J.A.L., 2002. The role of ethylene and wound signaling in resistance of tomato to *Botrytis cinerea*. Plant Physiol. 129, 1341-1351.

Dixon, R.A., 2001. Natural products and plant disease resistance. Nature 411, 843-847.

Dixon, R.A., Achnine, L., Kota, P., Liu, C.J., Reddy, M.S.S., Wang, L.J., 2002. The phenylpropanoid pathway and plant defence - a genomics perspective. Mol. Plant Pathol. 3, 371-390.

El Hadrami, A., Adam, L.R., Daayf, F. 2011. Biocontrol treatments confer protection against Verticillium dahliae infection in potato by inducing anti-microbial metabolites. Mol. Plant-Microbe Interact. 24, 328-335.

Facchini, P.J., Hagel, J., Zulak, K.G., 2002. Hydroxycinnamic acid amide metabolism: physiology and biochemistry. Can. J. Bot. 80, 577-589.

Fayos, J., Bellés, J.M., López-Gresa, M.P., Primo, J., Conejero, V., 2006. Induction of gentisic acid 5-*O*-β-D-xylopyranoside in tomato and cucumber plants infected by different pathogens. Phytochemistry 67, 142-148.

Fleming, A.J., Mandel, T., Roth, I., Kuhlemeier, C., 1993. The patterns of gene expression in the tomato shoot apical meristem. Plant Cell 5, 297-309

Fuentes-Alventosa, J.M., Rodriguez, G., Cermeno, P., Jimenez, A., Guillen, R., Fernandez-Bolanos, J., Rodriguez-Arcos, R., 2007. Identification of flavonoid diglycosides in several genotypes of asparagus from the Huétor-Tájar population variety. J. Agric. Food Chem. 55, 10028-10035.

Hagel, J.M., Facchini, P.J., 2005. Elevated tyrosine decarboxylase and tyramine hydroxycinnamoyltransferase levels increase wound-induced tyramine-derived hydroxycinnamic acid amide accumulation in transgenic tobacco leaves. Planta 221, 904-914.

Hagemeier, J., Schneider, B., Oldham, N.J., Hahlbrock, K., 2001. Accumulation of soluble and wall-bound indolic metabolites in *Arabidopsis thaliana* leaves infected with Virulent or avirulent *Pseudomonas syringae* pathovar *tomato* strains. Proc. Natl. Acad. Sci. U. S. A. 98, 753-758.

He, X.Z., Dixon, R.A., 2000. Genetic manipulation of isoflavone 7-*O*-methyltransferase enhances biosynthesis of 4'-*O*-methylated isoflavonoid phytoalexins and disease resistance in alfalfa. Plant Cell 12, 1689-1702.

Hirota, A., Taki, S., Kawaii, S., Yano, M., Abe, N., 2000. 1,1-diphenyl-2-picrylhydrazyl radical-scavenging compounds from soybean miso and antiproliferative activity of isoflavones from soybean miso toward the cancer cell lines. Biosci. Biotechnol. , Biochem. 64, 1038-1040.

Hoffmann, L., Besseau, S., Geoffroy, P., Ritzenthaler, C., Meyer, D., Lapierre, C., Pollet, B., Legrand, M., 2004. Silencing of hydroxycinnamoyl-coenzyme A shikimate/quinate hydroxycinnamoyltransferase affects phenylpropanoid biosynthesis. Plant Cell 16, 1446-1465.

Jahangir, M., Abdel-Farid, I.B., Kim H.K., Choi, Y.H.,Verpoorte, R. 2009. Healthy and unhealthy plants: The effect of stress on the metabolism of Brassicaceae. Environ. Exp. Bot. 67, 23-33.

Kang, K., Lee, K., Sohn, S.O., Park, S., Lee, S., Kim, S.Y., Kim, Y.S., Back, K., 2009. Ectopic expression of serotonin *N*-hydroxycinnamoyltransferase and differential production of phenylpropanoid amides in transgenic tomato tissues. Scientia Horticulturae 120, 504-510.

Keller, H., Hohlfeld, H., Wray, V., Hahlbrock, K., Scheel, D., Strack, D., 1996. Changes in the accumulation of soluble and cell wall-bound phenolics in elicitor-treated cell suspension cultures and fungus-infected leaves of *Solanum tuberosum*. Phytochemistry 42, 389-396.

King, R.R., Calhoun, L.A., 2005. Characterization of cross-linked hydroxycinnamic acid amides isolated from potato common scab lesions. Phytochemistry 66, 2468-2473.

Lee, SW., Robb, J., Nazar, RN., 1992. Truncated phenylalanine ammonia-lyase expression in tomato. J. Biol. Chem. 267, 11824-11830.

Linthorst, H.J.M., 1991. Pathogenesis-related proteins of plants. Crit. Rev. Plant Sci. 10, 123-150.

López-Gresa, M.P., Maltese, F., Bellés, J.M., Conejero, V., Kim, H.K., Choi, Y.H., Verpoorte, R, 2010. Metabolic response of tomato leaves upon different plant-pathogen interactions. Phytochem Anal 21, 89-94

Lund, S.T., Stall, R.E., Klee, H.J., 1998. Ethylene regulates the susceptible response to pathogen infection in tomato. Plant Cell 10, 371-382.

Matsuda, F., Miyagawa, H., Ueno, T., 2000. Absolute structure of *N-p*-coumaroyloctopamine in elicitor-treated potato tuber tissue. Biosci. Biotechnol. Biochem. 64, 625-627.

Millar, D.J., Long, M., Donovan, G., Fraser, P.D., Boudet, A.M., Danoun, S., Bramley, P.M., Bolwell, G.P., 2007. Introduction of sense constructs of cinnamate 4-hydroxylase (CYP73A24) in transgenic tomato plants shows opposite effects on flux into stem lignin and fruit flavonoids. Phytochemistry 68, 1497-1509.

Muhlenbeck, U., Kortenbusch, A., Barz, W., 1996. Formation of hydroxycinnamoylamides and α-hydroxyacetovanillone in cell cultures of *Solanum khasianum*. Phytochemistry 42, 1573-1579.

Nawrath, C., Métraux, J.P., 1999. Salicylic acid induction-deficient mutants of Arabidopsis express PR-2 and PR-5 and accumulate high levels of camalexin after pathogen inoculation. Plant Cell 11, 1393-1404.

Newman, M.A., Von Roepenack-Lahaye, E., Parr, A., Daniels, M.J., Dow, J.M., 2001. Induction of hydroxycinnamoyl-tyramine conjugates in pepper by *Xanthomonas campestris,* a plant defense response activated by *hrp* gene-dependent and *hrp* gene-independent mechanisms. Mol. Plant-Microbe Interact. 14, 785-792.

Niggeweg, R., Michael, A.J., Martin, C., 2004. Engineering plants with increased levels of the antioxidant chlorogenic acid. Nat. Biotechnol. 22, 746-754.

Niyogi, K.K., Fink, G.R., 1992. Two anthranilate synthase genes in Arabidopsis: -defense-related regulation of the tryptophan pathway. Plant Cell 4, 721-733.

Pellegrini, L., Rohfritsch, O., Fritig, B., Legrand, M., 1994. Phenylalanine ammonia-lyase in tobacco. Molecular cloning and gene expression during the hypersensitive reaction to Tobacco Mosaic Virus and the response to a fungal elicitor. Plant Physiol. 106, 877-886.

Reinhardt, D., Wiemken, A., Boller, T., 1991. Induction of ethylene biosynthesis in compatible and incompatible interactions of soybean roots with *Phytophthora megasperma* f.sp. *glycinea* and its relation to phytoalexin accumulation. J. Plant Physiol. 138, 394-399.

Rodrigo, I., Vera, P., Tornero, P., Hernandez-Yago, J., Conejero, V., 1993. cDNA cloning of viroid-induced tomato pathogenesis-related protein P23. Characterization as a vacuolar antifungal factor. Plant Physiol. 102, 939-945.

Schilmiller, A.L., Stout, J., Weng, J.-K., Humphreys, J., Ruegger, M.O., Chapple, C., 2009. Mutations in the *cinnamate 4-hydroxylase* gene impact metabolism, growth and development in Arabidopsis. Plant J. 60, 771-782

Schmidt, A., Grimm, R., Schmidt, J., Scheel, D., Strack, D., Rosahl, S., 1999. Cloning and expression of a potato cDNA encoding hydroxycinnamoyl-CoA: Tyramine *N*-(hydroxycinnamoyl)transferase. J. Biol. Chem. 274, 4273-4280.

Smith-Becker, J., Marois, E., Huguet, E.J., Midland, S.L., Sims, J.J., Keen, N.T., 1998. Accumulation of salicylic acid and 4-hydroxybenzoic acid in phloem fluids of cucumber during systemic acquired resistance is preceded by a transient increase in phenylalanine ammonia-lyase activity in petioles and stems. Plant Physiol. 116, 231-238.

Tan, J.W., Bednarek, P., Liu, H.K., Schneider, B., Svatos, A., Hahlbrock, K., 2004. Universally occurring phenylpropanoid and species-specific indolic metabolites in infected and uninfected *Arabidopsis thaliana* roots and leaves. Phytochemistry 65, 691-699.

Tanaka, H., Nakamura, T., Ichino, K., Ito, K., 1989. A phenolic amide from *Actinodaphne longifolia*. Phytochemistry 28, 2516-2517.

Tornero, P., Rodrigo, I., Conejero, V., Vera, P., 1993. Nucleotide sequence of a cDNA encoding a pathogenesis related protein, P1-P14, from tomato (*Lycopersicon esculentum*). Plant Physiol. 102, 325.

Van Loon, L.C., Rep, M., Pieterse, C.M.J., 2006. Significance of inducible defense-related proteins in infected plants. Annu. Rev. Phytopathol. 44, 135-162.

Von Roepenack-Lahaye, E., Newman, M.A., Schornack, S., Hammond-Kosack, K.E., Lahaye, T., Jones,J.D.G., Daniels,M.J., Dow,J.M., 2003. *p*-coumaroylnoradrenaline, a novel plant metabolite implicated in tomato defense against pathogens. J. Biol. Chem. 278, 43373-43383.

Wolski, E.A., Henriquez, M.A., Adam L.R., Badawi M., Andreu A.B., El Hadrami, A, Daayf, F. 2010. Induction of defense genes and secondary metabolites in saskatoons (*Amelanchier alnifolia* Nutt.) in response to *Entomosporium mespili* using jasmonic acid and Canada milkvetch extracts. Environ. Exp. Bot. 68, 273-282.

Zacarés, L., López-Gresa, M.P., Fayos, J., Primo, J., Bellés, J.M., Conejero, V., 2007. Induction of *p*-coumaroyldopamine and feruloyldopamine, two novel metabolites, in tomato by the bacterial pathogen *Pseudomonas syringae*. Mol. Plant-Microbe Interact. 20, 1439-1448.

Figure 1. A) Accumulation of *cis/trans* isomers of *N*-*p*-coumaroylnoradrenaline (CNA), *N*-feruloylnoradrenaline (FNA) (left panel), and *N*-*p*-coumaroyloctopamine (CO), *N*-feruloyloctopamine (FO) (right panel) in Rutgers tomato leaves at the specified times (h) after inoculation with *Pseudomonas syringae* pv. *tomato* at 10^7 CFU ml^{-1}. B) Accumulation of chlorogenic acid (CGA) (left panel), and rutin (right panel) in control and infected Rutgers tomato leaves at the specified times (h) after inoculation with *Pseudomonas syringae* pv. *tomato* at 10^7 CFU ml^{-1} (*Pst*). Results are means ± s.e. of three independent biological replicates.

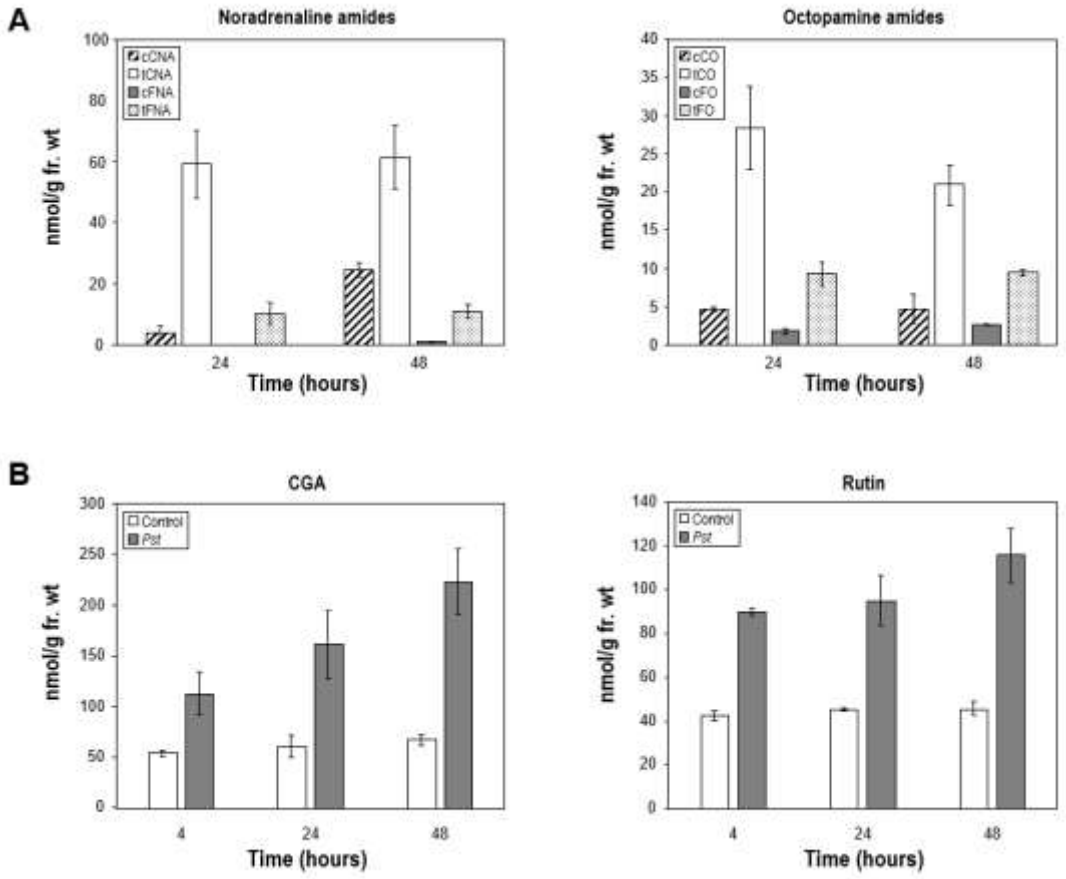

Figure 2. A) Accumulation of *cis/trans* isomers of *N*-*p*-coumaroylnoradrenaline (CNA), *N*-feruloylnoradrenaline (FNA) (left panel), and *N*-*p*-coumaroyloctopamine (CO), *N*-feruloyloctopamine (FO) (right panel) in transgenic NahG tomato leaves at the specified times (h) after inoculation with *Pseudomonas syringae* pv. *tomato* at 10^7 CFU ml^{-1}. B)

Accumulation of chlorogenic acid (CGA) (left panel), and rutin (right panel) in control and infected transgenic NahG tomato leaves at the specified times after inoculation with *Pseudomonas syringae* pv. *tomato* at 10^7 CFU ml^{-1} (*Pst*). Results are means ± s.e. of three independent biological replicates.

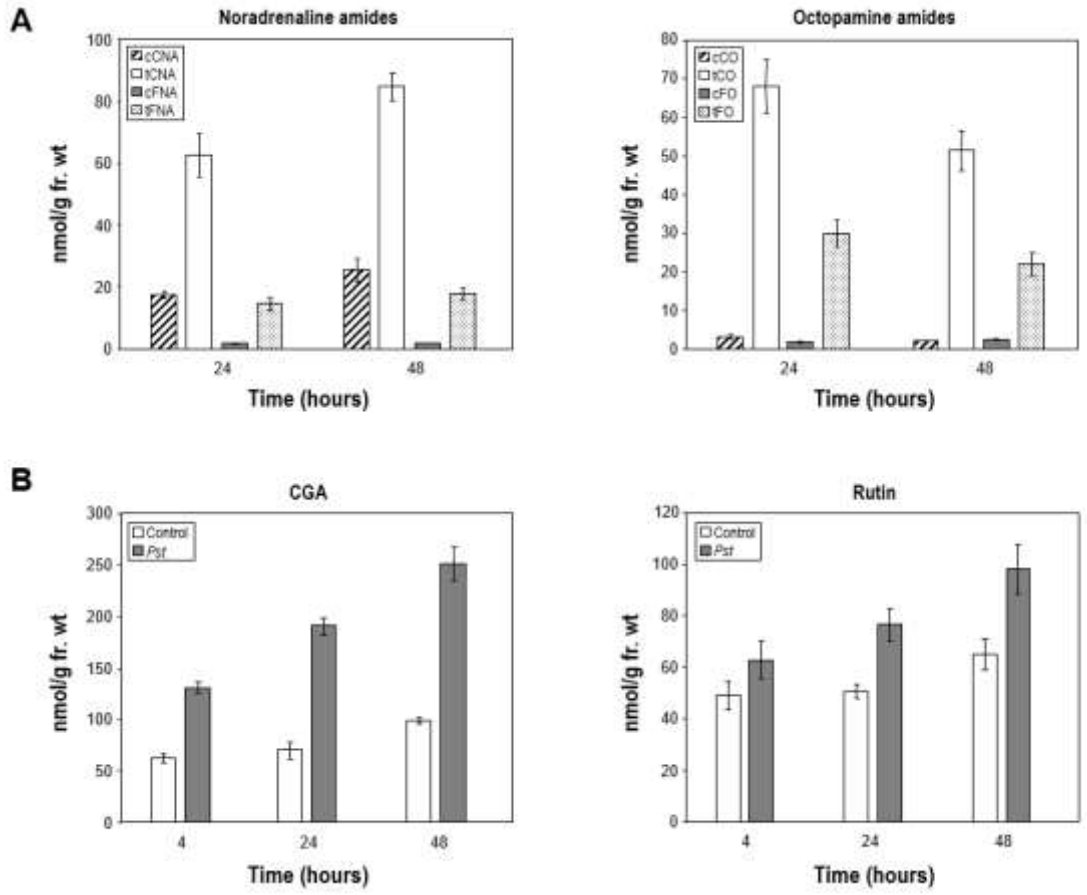

Figure 3. A) Accumulation of *cis/trans* isomers of *N-p*-coumaroylnoradrenaline (CNA), *N*-feruloylnoradrenaline (FNA) (left panel), and *N-p*-coumaroyloctopamine (CO), *N*-feruloyloctopamine (FO) (right panel) in Rutgers tomato plants exposed to exogenous ethylene. Plants were treated with either air (control) or 50 µl l^{-1} ethylene at a constant flow of 15 l h^{-1} during 24 h and then samples collected for hydroxycinnamic amides analysis. B) Accumulation of chlorogenic acid (CGA) (left panel), and rutin (right panel) in control and Rutgers tomato plants exposed to exogenous ethylene.

Plants were treated with either air (control) or 50 µl l^{-1} ethylene at a constant flow of 15 l h^{-1} during 24 h, and samples were collected at the specified times. Results are means ± s.e. of three independent biological replicates.

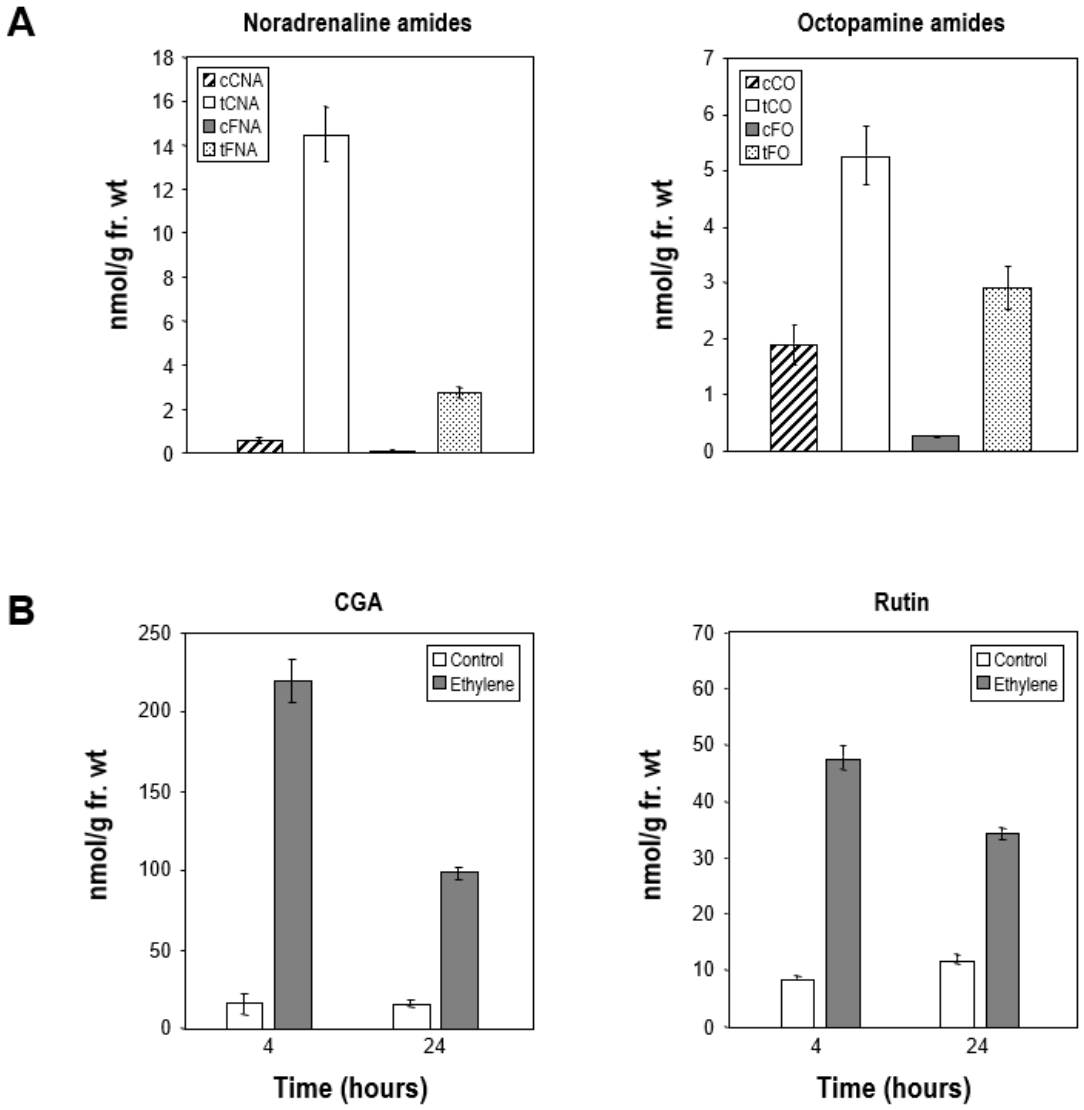

Figure 4. Effect of 1 mM 2-aminoethoxyvinylglycine (AVG) treatment on *cis/trans N-p*-coumaroylnoradrenaline (CNA), *N*-feruloylnoradrenaline (FNA), *N-p*-coumaroyloctopamine (CO), and *N*-feruloyloctopamine (FO) accumulation in Rutgers tomato leaves inoculated with 10^7 CFU ml^{-1} *Pseudomonas syringae* pv. *tomato* at 24 and 48 h postinoculation Values are the mean ± s.e. from three independent biological replicates.

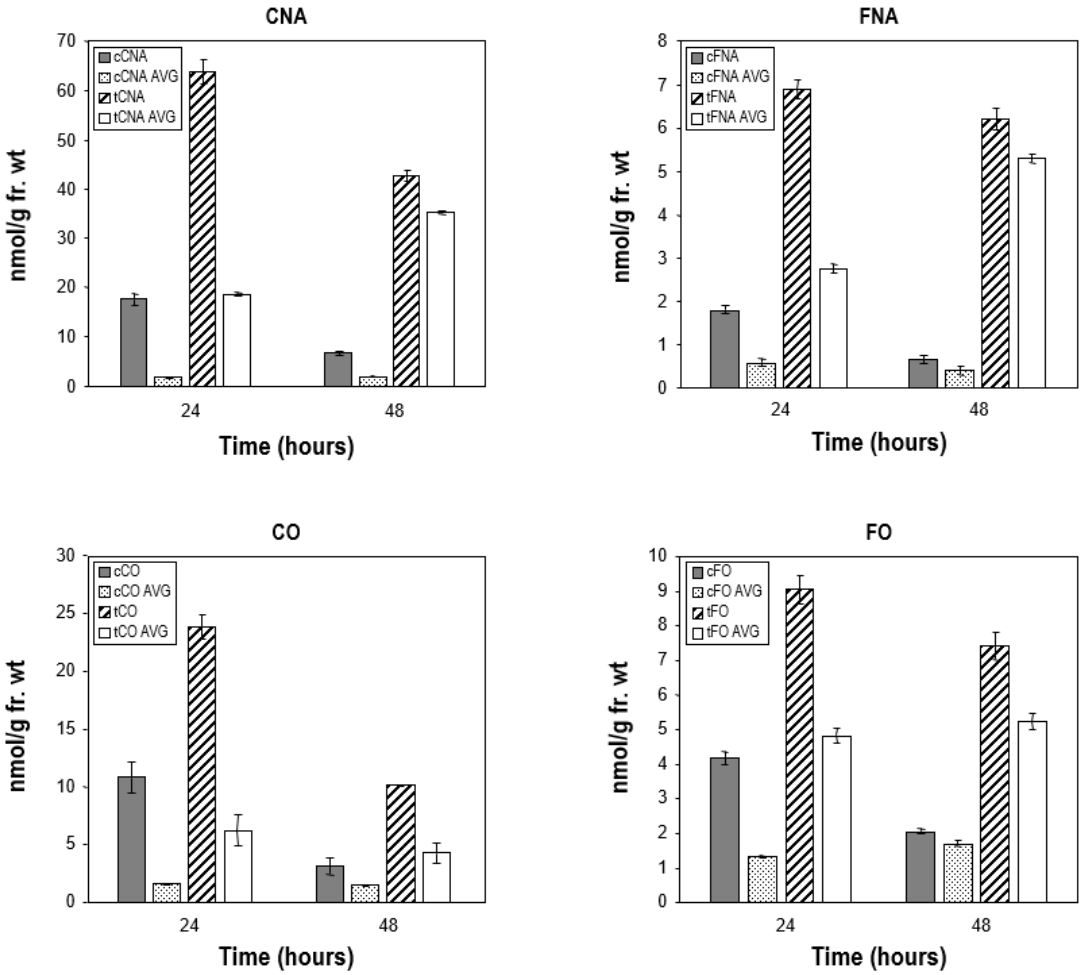

Figure 5. Accumulation of *PAL*, *C4H* and *HQT* mRNAs in Rutgers tomato leaves upon infection with *Pseudomonas syringae* pv. *tomato* or mock-inoculated with 10 mM $MgSO_4$. Time points indicated are in hours. Fifteen µg of total RNA isolated from Rutgers tomato leaves were separated on formaldehyde gels, transferred to nylon membranes, and probed for the presence of the transcripts of *PAL*, *C4H*, and *HQT* in both mock-inoculated and bacterial infiltrated tomato leaves. Ethidium bromide stained RNAs are shown as a loading control.

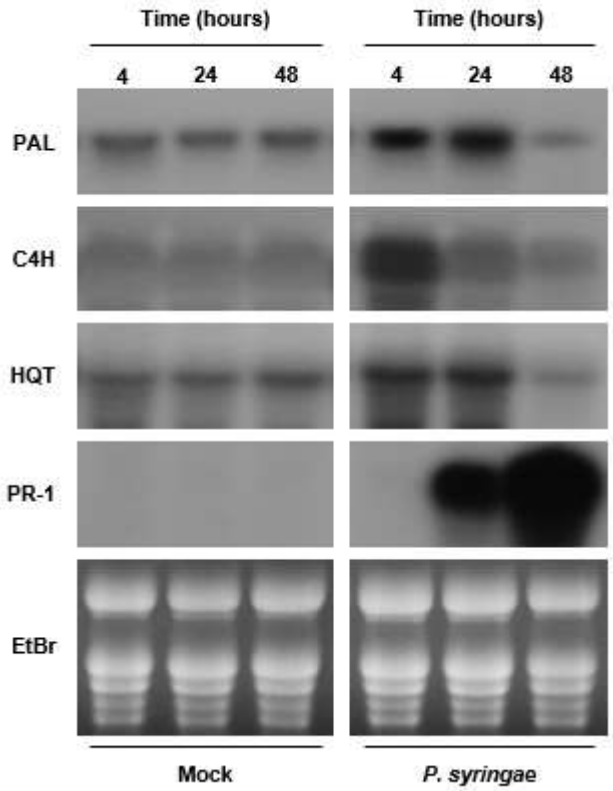

Figure S1. A) Representative reverse-phase C18 HPLC-PDA absorbance chromatogram analysed at 320 nm from soluble methanol extracts of mock-inoculated and infected tomato leaves. Leaves were mock-inoculated or infiltrated with *Pseudomonas syringae* pv. *tomato* at 10^7 CFU ml^{-1} and samples were colleted at 24 h after bacterial infiltration of the leaflets. Absorbance was monitored by a photodiode array detector with a range of maxplot between 240 and 400 nm and a spectral resolution of 1.2 nm. Peaks 1-8 show the induced secondary metabolites with retention times of 9.6, 11.3, 11.6 11.8, 12.3, 13.2, 13.6, and 13.9 min, respectively. B) Representative reverse-phase C18 HPLC-MS chromatograms from the same soluble methanol extracts. Single ion chromatograms extracted from total ion current of *m/z* species of 314, 344, 298, and 328.

Table S1. Electrospray ionization mass spectra, UV absorbance maxima and HPLC retention times comparisons[a]

	Compounds							
	2	3	4	5	2A	3A	4A	5A
Negative ions[b]								
$[M-H]^-$	314.1 (100)	344.2(100)	298.1 (100)	328.1 (100)	314.1 (100)	344.2 (100)	298.1 (100)	328.1 (100)
Positive ions[b]								
$[M+H]^+$	316.3 (50)	346.4 (30)	300.4 (40)	330.3 (60)	316.3 (55)	346.3 (10)	300.3 (25)	330.4(25)
$[M+H-H_2O]^+$	298.3 (100)	328.4 (100)	282.3 (100)	312.4 (100)	298.3 (100)	328.3 (100)	282.4 (100)	312.4 (100)
(m/z)	147.2 (45)	177.2 (25)	147.3 (25)	177.1 (20)	147.2 (30)	177.3 (40)	147.3 (50)	177.1 (10)
Negative ions[c]								
$[M-H]^-$	314.1 (100)	344.1 (100)	298.2 (100)	328.2 (100)	314.2 (100)	344.1 (100)	298.2 (100)	328.2 (100)
Positive ions[c]								
$[M+H]^+$	316.4 (15)	346.4 (15)	300.4 (25)	330.4 (10)	316.4 (20)	346.4 (20)	300.3 (50)	330.3 (60)
$[M+H-H_2O]^+$	298.4 (100)	328.4 (100)	282.4 (100)	312.4 (100)	298.3 (100)	328.3 (100)	282.3 (100)	312.3 (100)
(m/z)	147.2 (40)	177.3 (30)	147.2 (35)	177.3 (45)	147.2 (50)	177.3 (30)	147.2 (20)	177.3 (20)
λ_{max}[b] (nm)	292, 310	290, 319	290, 310	290, 319	276, 309	278, 305	276, 304	279, 308
λ_{max}[c] (nm)	292, 310	290, 319	290, 310	290, 319	277, 306	279, 306	273, 305	274, 302
RT[b] (min)	11.3	11.6	11.8	12.3	10.2	10.4	10.6	10.8
RT[c] (min)	11.4	11.7	11.8	12.4	10.3	10.5	10.7	11.0

[a] Negative and positive ion detection mode (m/z [%]), UV absorbance maxima (λ max) and retention times (RT).
[b] Results of peaks **2**-5 and **2A**-5A of methanol extracts from Rutgers tomato leaves infected with *Pseudomonas syringae* pv *tomato*
[c] Results of synthetic HCAA.

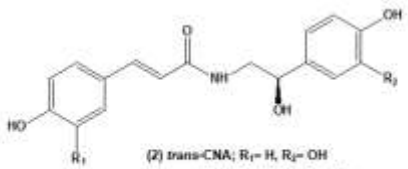

(2) trans-CNA; R_1= H, R_2= OH
(3) trans-FNA; R_1= OCH_3, R_2= OH
(4) trans-CO; R_1= H, R_2= H
(5) trans-FO; R_1= OCH_3, R_2= H

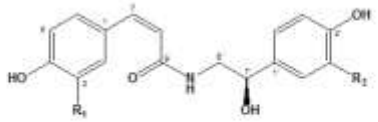

(2A) cis-CNA; R_1= H, R_2= OH
(3A) cis-FNA; R_1= OCH_3, R_2= OH
(4A) cis-CO; R_1= H, R_2= H
(5A) cis-FO; R_1= OCH_3, R_2= H

Figure S2. Expression of *PR1* and *P23* transcripts in Rutgers tomato leaves upon infection with *Pseudomonas syringae pv. tomato* or treatment with chlorogenic acid (CGA) with the corresponding controls. A: *PR1* and *P23* mRNA accumulation in *P. syringae*-infected tomato leaves. B: *PR1* and *P23* mRNA accumulation in tomato leaves incubated with 1 mM CGA. Samples were collected at the specified time points (h) after the beginning of the treatment. Total RNA from *P. syringae*-infected tomato leaves or treated with 1 mM CGA with the corresponding controls was prepared and reverse-transcribed using *PR1*- and *P23*-specific primers. The accumulation of *PRL2* transcript was used as a control. The resulting RT-PCR products were separated on 1% agarose gels. The gels were stained with ethidium bromide and visualised under UV light. Equivalent results were obtained in two separate experiments.

Table S2: ^{1}H and $^{13}CNMR$ data of compounds **2A**, and **2** in MeOH-d_4

	2A		**2**	
Position	δ C[a] (*m*)[c]	δ H[a] (*m*, *J* Hz)	δ C[b] (*m*)[c]	δ H[b] (*m*, *J* Hz)
1	130.6[d] (*s*)	-	127.8 (*s*)	-
2	132.4 (*d*)	7.40 (*d*, 8.6)	130.6 (*d*)	7.41 (*d*, 8.6)
3	116.2 (*d*)	6.72 (*d*, 8.6)	116.7 (*d*)	6.79 (*d*, 8.6)
4	161.2[d] (*s*)	-	160.6 (*s*)	-
5	116.2 (*d*)	6.72 (*d*, 8.6)	116.7 (*d*)	6.79 (*d*, 8.6)
6	132.4 (*d*)	7.40 (*d*, 8.6)	130.6 (*d*)	7.41 (*d*, 8.6)
7	138.6 (*d*)	6.62 (*d*,12.6)	142.0 (*d*)	7.46 (*d*,15.7)
8	121.1 (*d*)	5.81 (*d*,12.6)	118.4 (*d*)	6.42 (*d*,15.7)
9	170.2[d] (*s*)	-	169.6 (*s*)	-
1'	130.7[d] (*s*)	-	135.6 (*s*)	-
2'	114.4 (*d*)	6.84 (*d*, 1.7)	114.4 (*d*)	6.85 (*d*, 1.6)
3'	146.3[d] (*s*)	-	146.3* (*s*)	-
4'	145.9[d] (*s*)	-	146.0* (*s*)	-
5'	116.1 (*d*)	6.72 (*d*, 8.1)	116.2 (*d*)	6.75 (*d*, 8.2)
6'	118.8 (*d*)	6.68 (*dd*, 8.1, 1.7)	118.8 (*d*)	6.73 (*dd*, 8.2, 1.6)
7'	73.4 (*d*)	4.62 (*dd*, 7.8, 4.9)	73.6 (*d*)	4.65 (*dd*, 7.7, 4.9)
8'	47.8 (*t*)	3.46 (*dd*, 13.8, 4.9) 3.36 (*dd*, 13.8, 7.8)	47.8 (*t*)	3.51 (*dd*, 13.5, 4.9) 3.41 (*dd*, 13.5, 7.7)

[a] Bruker DRX 600 MHz.
[b] Bruker AV 300 MHz.
[c] Multiplicity deduced by DEPT.
[d] Assignments made by HMBC experiments.
*Interchangeable assignments

Table S3. Free radical scavenging activities of hydroxycinnamic acids, β-phenylethyl-amines, HCAA, and natural antioxidant metabolites. Values of 2,2-diphenyl-1-picrylhydrazyl (DPPH) scavenging activity represent the concentration of product necessary to reduce to 50% the absorbance of DPPH (ED_{50}), and are means ± standard error of three individual independent experiments.

Table S3. Antioxidant activity of hydroxycinnamic acids, β-phenylethyl-amines, hydroxycinnamic acid amides (HCAA), and natural antioxidant metabolites.

Compound	ED_{50} (μM)
p-coumaric acid	>200
Ferulic acid	44.92 ± 0.06
Noradrenaline	24.10 ± 0.16
Octopamine	>200
trans-*p*-coumaroylnoradrenaline	43.32 ± 0.48
trans-feruloylnoradrenaline	7.92 ± 0.01
trans-*p*-coumaroyloctopamine	>200
trans-feruloyloctopamine	81.11 ± 0.08
Chlorogenic acid	26,00 ± 0,05
Rutin	20,64 ± 0,08
Quercetin	14.56 ± 0.03
Ascorbic acid	73.52 ± 0.28
Tocopherol	31.27 ± 0.71
Gentisic acid	66.62 ± 0.11
Resveratrol	112.99 ± 1.53
BHT	61.13 ± 0.02